ISBN: 978-3-95450-132-8 doi:10.18429/JACoW-IPAC2014-TUPRI019

INCOHERENT AND COHERENT EFFECTS OF SPACE CHARGE LIMITED ELECTRON CLOUDS

F. B. Petrov, O. Boine-Frankenheim, O. S. Haas, TEMF, TU-Darmstadt, Germany

Abstract

Recent studies show that the space charge limited (saturated) electron cloud generated by relativistic bunches has strongly inhomogeneous distribution. In particular, a dense electron sheath is formed near the pipe wall. This feature modifies the stopping powers and the microwave transmission compared with the uniform cloud case. In this paper we investigate further the influence of the space charge limited electron cloud on relativistic bunches. In particular, we focus on the incoherent tune spread and compare the results with the homogeneous cloud case. We derive analytical expressions governing the pinch dynamics of the saturated cloud in round geometry. The contribution of the electron cloud sheath to the wake fields is investigated as well. Findings of the analytical theory are then successfully compared with numerical particle-in-cell simulations.

INTRODUCTION

Electron clouds introduce diverse limitations on the performance of modern and future accelerators [1]. They lead to cryogenic heat load, pressure rise, emittance growth, synchronous phase shift and coherent beam instabilities. The last three effects depend on the wakefields induced by bunches in an electron cloud.

In the present paper we continue to study of how the saturated electron clouds affect relativistic proton bunches. In the first section we address the contribution of an electron cloud sheath to the longitudinal wakefields. Such kind of sheath was found to be formed at the saturation of the electron cloud buildup under the LHC conditions [3]. In the second section the studies of the tune shifts induced by electron clouds are presented. The possible influence on the electron cloud density measurements is also discussed.

RADIALLY SYMMETRIC PINCH AND WAKEFIELDS

In Ref. [2, 3] it was pointed out that in some cases at saturation the electron cloud density at the pipe wall is significantly larger than the density in the pipe center, i.e. a dense electron cloud sheath is formed near the wall. It was shown that the wakefields induced by this distribution differ from the uniform cloud case. In this section we investigate the pinch of a ring-like electron cloud and the longitudinal wakefield induced by such an electron cloud distribution.

If the beam pipe is cylindrical and the bunch is sufficiently short and centered, then electrons at distance R_0 from pipe center receive a transverse velocity kick (See Ref. [4]):

$$v \approx \frac{1}{c}\int_{-\infty}^{z} \frac{e^2\lambda_i(z)}{2\pi\epsilon_0 R_0 m_e} dz, \qquad (1)$$

where c is the velocity of light, e is the electron charge, λ_i is the beam line density, ϵ_0 is the vacuum permittivity, m_e is the electron mass, z is the coordinate along the pipe. For a Gaussian longitudinal bunch distribution this kick is

$$v(z) = R(z)'c = \frac{1}{c}\frac{e^2 N_i}{4\pi\epsilon_0 R_0 m_e}\left(1 + \mathrm{erf}\left[\frac{z}{\sqrt{2}\sigma_z}\right]\right), \qquad (2)$$

where N_i is the bunch population, σ_z is the bunch length. The electron distance to the pipe center is then governed by

$$R(z) = R_0 - \frac{1}{c}\int_{-\infty}^{z} v ds = \\ = R_0 - \frac{1}{c^2}\frac{e^2 N_i}{4\pi\epsilon_0 R_0 m_e}\left(z + z\mathrm{erf}\left[\frac{z}{\sqrt{2}\sigma_z}\right] + \sqrt{\frac{2}{\pi}}\sigma_z e^{-\frac{z^2}{2\sigma_z^2}}\right). \qquad (3)$$

If the pinch dimension is much larger longitudinally than transversely, which is typically the case, then the electron cloud potential at the center is governed approximately by the local transverse charge distribution:

$$\phi(z) \approx \frac{e\lambda_e}{2\pi\epsilon_0}\ln\left(\frac{R(z)}{R_0}\right). \qquad (4)$$

One can then obtain the longitudinal electric field of the ring-like charge distribution at the pipe center:

$$E_z(z) = -\frac{\partial\phi(z)}{\partial z} = -\frac{e\lambda_e}{2\pi\epsilon_0}\frac{R'(z)}{R(z)} \qquad (5)$$

For Gaussian and rectangular bunch shapes this field can be calculated analytically.

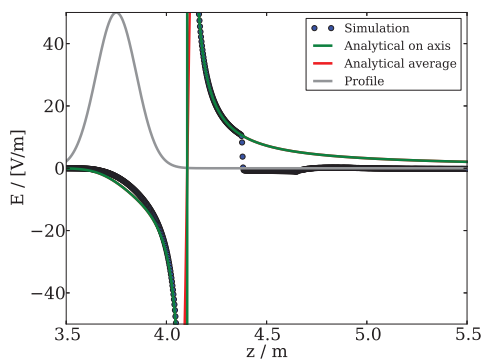

Figure 1: (Color) Electric field of the ring-like electron cloud under the influence of the passing proton bunch. $N_i = 2\times10^{11}$, $\sigma_z = 10$ cm and $R_0 = 2$ cm.

Fig. 1 shows the analytical and numerical longitudinal wakefields on the pipe axis for two different bunch populations for the ring-like electron cloud distribution. One

ISBN: 978-3-95450-132-8 doi:10.18429/JACoW-IPAC2014-TUPRI019

Table 1: Simulation parameters for the LHC-like bunches.

Bunch length, σ_z [m]	0.1
Bunch radius, σ_r [m]	10^{-3}
Bunch population, N_i	$2.5\times10^{10} - 6\times10^{11}$
Bunch spacing [ns]	25
Pipe radius, R_p [m]	2×10^{-2}
Magnetic field, B [T]	0.1
Maximum total SEY, δ_{max}	1.4
Energy of δ_{max}, $W_{SEY,max}$ [eV]	250
Reflection probability	1.0
Rediffusion probability, δ_{rd}	0.7
Ring circumference, C [m]	2.7×10^{4}
Fraction of the ring with EC	0.1
Betatron tunes Q_x/Q_y	65.32/63.27
Lorentz factor, γ_0	450

can see that the simulations predict nearly the same field that, however, abruptly cancels behind the bunch due to the electron cloud loss at the wall. Integrating Eq. 5 over R_0 one can obtain a wakefield for a cloud with a finite thickness d and density ρ_e. This is the subject of our future studies.

INCOHERENT TUNE SHIFT DUE TO SATURATED ELECTRON CLOUD

In this section we analyze the effect of the saturated electron cloud on the bunch tune distribution. For this purpose, firstly, we perform buildup simulations until the saturation of the electron cloud is reached. The buildup starts from the initially uniform electron cloud. No primary electrons are produced during the buildup. Secondly, we use the obtained electron cloud profiles to track the beam particles and calculate the corresponding tune shifts. In these calculation we neglect the synchrotron motion and assume a simple constant focusing lattice. The resulting tune shifts are compared with the uniform electron cloud models. Average or central densities of the realistic electron cloud are assigned to the uniform clouds. In all the simulations we study the simplified case of the circular geometry similar to the LHC beam pipe. The simulation parameters are listed in Table 1.

Fig. 2 shows the average and central electron cloud densities versus the bunch population. The curves are accompanied by the evolution of the heat load. The heat load is calculated for the saturated cloud as energy deposited on the wall during one bunch passage divided by the bunch spacing. In the studied case one can see that the average electron cloud density has a maximum around 1.5×10^{11} particles per bunch. On the contrary, the central density reaches minimum at 3×10^{11}. At this point the cloud is mainly distributed into two vertical stripes. Further increase of intensity leads to the formation of another stripe in the middle of the pipe and, thus, the growing central density.

Fig. 4 and Fig. 5 show the average tune shift induced by the realistic and two chosen uniform clouds as a function of

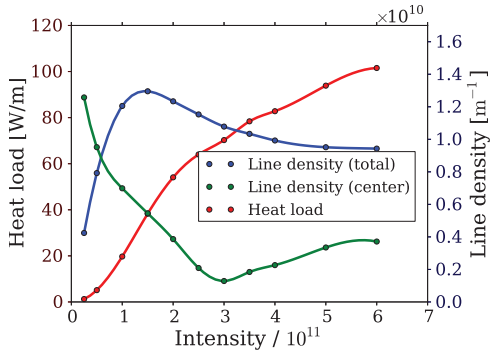

Figure 2: (Color) The saturated average electron cloud line density (blue), central density (green) and heat load (red) against the bunch population in the presence of external dipole magnetic field. The SEY is chosen as δ_{max}=1.4.

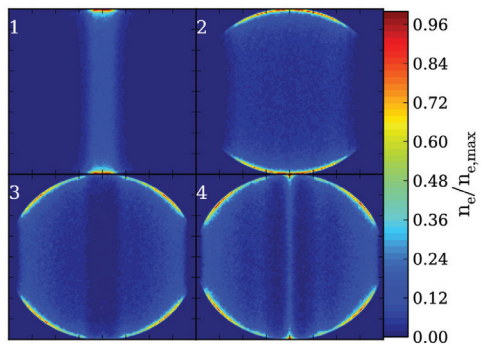

Figure 3: (Color) Electron cloud density snapshot $6\sigma_z$ before the bunch. Intensities are 2.5×10^{10}, 10^{11}, 3×10^{11} and 6×10^{11} correspondingly. Densities are normalized to the maximum.

intensity. It is important to notice the $N_i = 3\times10^{11}$ case (See Fig. 3). When two dense stripes are formed, the tune shift becomes negative in one direction and positive in another direction. Both of the uniform cloud models give positive tune shifts. It is also worth noting that all the models give dissimilar dependence of the tune shift and the tune spread on the bunch population.

The measurements of the electron cloud density based on the tune shift typically utilize the following formula:

$$\bar{\rho} = \frac{\gamma_0}{r_e L}\left(\frac{\Delta Q_x}{\bar{\beta}_x} + \frac{\Delta Q_y}{\bar{\beta}_y}\right), \qquad (6)$$

where $\bar{\rho}$ is the average electron cloud density along the bunch, γ_0 is the Lorentz factor, r_e is the electron classical radius, L is the circumference, ΔQ_x and ΔQ_y are the horizontal and vertical measured tune shifts, $\bar{\beta}_x$ and $\bar{\beta}_y$ are the average horizontal and vertical beta-functions. In case of two stripes the tune shift contributions in horizontal and vertical plane nearly cancel and give approximately zero density. This happens in agreement with the Poisson equation for zero charge density: $\partial E_x/\partial x = -\partial E_y/\partial y$. Similar electron distributions are very common in accelerators (See for example

ISBN: 978-3-95450-132-8 doi:10.18429/JACoW-IPAC2014-TUPRI019

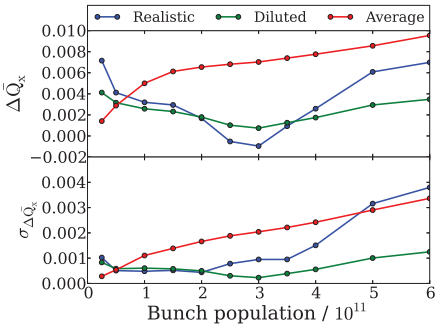

Figure 4: (Color) Average horizontal tune shift and tune spread as a function of bunch population. The blue curves shows the results for the realistic cloud. The green curve shows the results for the uniform, diluted cloud. The red curve corresponds to the uniform cloud.

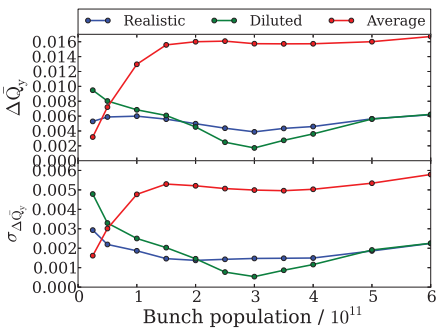

Figure 5: (Color) Average vertical tune shift and tune spread as a function of bunch population. The blue curves shows the results for the realistic cloud. The green curve shows the results for the uniform, diluted cloud. The red curve corresponds to the uniform cloud.

Refs. [5,6]). Thus, the measurements of the tune shift would mainly include only the information about the central density in field-free regions.

Fig. 6 shows the electron cloud densities averaged along the bunch and reconstructed using Eq. 6. One can observe that the dissimilarity between the realistic and diluted models almost disappears. The values are larger than given in

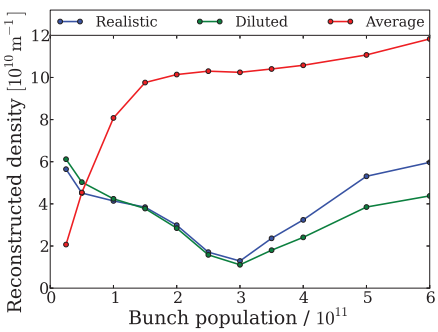

Figure 6: (Color) Electron cloud density in the dipole region reconstructed from tune shifts using Eq. 6.

Fig. 2 because of the electron cloud pinch. One can see, as well, that the densities get more amplified for higher intensities because more electrons are getting involved into pinch. At the same time the discrepancy between the diluted and realistic models after $N_i = 3 \times 10^{11}$ starts to grow and reaches 30%. This happens because in the realistic case the electron cloud density increases towards the wall, whereas the diluted model has a uniform distribution.

CONCLUSION AND OUTLOOK

We have studied the transverse and longitudinal effects of the saturated electron clouds in circular pipe geometry. Using the kick approximation we obtained the longitudinal wakefields for the ring-like electron cloud distribution. The resulting analytical expressions were successfully compared with the simulations. In future these expressions can be extended for the case of a thick electron cloud sheath.

A phenomenological study of the incoherent tune shifts due to the saturated electron cloud was performed for a broad intensity range. We focused on the electron cloud in an external dipole magnetic field. In most of the studied cases a significant difference between the horizontal and vertical tune shifts depending on the model can be observed.

In case of the "two-stripe" distribution and in agreement with the Poisson equation, our simulations give the horizontal and vertical tune shifts of the opposite signs. In the extreme case, the contribution of such distribution to the density measurements can become zero. In the meantime, uniform cloud models always yield positive tune shifts.

However, when horizontal and vertical tune shifts are used to extract the electron cloud density, the diluted and realistic models give nearly the same results for $N_i < 3\times10^{11}$. Under the studied conditions, the features of the realistic saturated electron cloud start to play role for $N_i \geq 3 \times 10^{11}$. On the contrary, the average cloud model gives almost always incorrect results.

ACKNOWLEDGMENT

Work is supported by the BMBF contract 05H12RD7.

REFERENCES

[1] F. Zimmermann, Phys. Rev. ST Accel. Beams 7, 124801 (2004)

[2] O. Haas, O. Boine-Frankenheim, and F. Petrov, Nuclear Instruments and Methods in Physics Research A 729 (2013) 290–295

[3] O. Boine-Frankenheim, E. Gjonaj, F. Petrov, F. Yaman, T. Weiland, and G. Rumolo, Phys. Rev. ST Accel. Beams 15, 054402 (2012)

[4] J. S. Berg, LHC Project Note 97, 1 July 1997

[5] P. He, M. Blaskiewicz, W. Fischer, BNL-81973-2009-IR

[6] J.M. Jimenez et al, Proceedings of the 2003 Particle Accelerator Conference, TOPC003, Portland, USA (2003) p. 307